Novel Fabry-Perot interferometer measurements of F-region ion temperature

K. Cierpka,[1] M. J. Kosch,[2,3] H. Holma,[4] A. J. Kavanagh,[2] and T. Hagfors[1]

Received 8 July 2002; revised 10 December 2002; accepted 26 December 2002; published 21 March 2003.

[1] Novel optical measurements of F-region ion temperatures have been made in conjunction with thermospheric neutral temperatures. A ground-based Fabry-Perot interferometer has been used to observe high-latitude F-region ion temperatures using the $O^+(^2P)$ auroral emission at 732 nm, and upper-thermospheric neutral temperatures using the $O(^1D)$ airglow emission at 630 nm. Dual wavelength measurements were made during February 2001 and clearly show that the ion temperature is equal to or greater than the neutral temperature, as expected. EISCAT radar measurements show that there is good agreement between the incoherent scatter and optical Doppler broadening methods of inferring ion temperature. *INDEX TERMS:* 2494 Ionosphere: Instruments and techniques; 2407 Ionosphere: Auroral ionosphere (2704); 2467 Ionosphere: Plasma temperature and density. **Citation:** Cierpka, K., M. J. Kosch, H. Holma, A. J. Kavanagh, and T. Hagfors, Novel Fabry-Perot interferometer measurements of F-region ion temperature, *Geophys. Res. Lett.*, *30*(6), 1293, doi:10.1029/2002GL015833, 2003.

1. Introduction

[2] Optical Doppler measurements of high-latitude F-region ion drift velocities, using the $O^+(^2P)$ multiplet emission at 732 nm, have been made from the ground [*Meriwether et al.*, 1974; *Smith et al.*, 1982; *Smith et al.*, 1985] and space [*Carr et al.*, 1992]. The discovery of this emission was first published in 1957 [*Sivjee et al.*, 1979]. $O^+(^2P)$ ions are primarily produced in the atmosphere by photo-ionisation of neutral atomic oxygen by solar EUV radiation at wavelengths less than 66.6 nm [*Carr et al.*, 1992]. A secondary source of $O^+(^2P)$ ions is electron impact ionisation with a threshold energy of 18.61 eV [*Carr et al.*, 1992]. This condition is satisfied at high latitudes in high altitude auroras produced by low energy (< 1 keV) particle precipitation [*Smith et al.*, 1982; *Omholt*, 1957].

[3] $O^+(^2P)$ ions are lost either by quenching or spontaneous photon emission. The emission is the result of the metastable transition between the excited ^2P and ^2D states of O^+ ions [*Carr et al.*, 1992]. The metastable $O^+(^2P)$ ions have a lifetime of 4.57 s [*Carr et al.*, 1992], which gives enough time to thermalise the ions [*Omholt*, 1957]. Modelling shows that the 732 nm volume emission covers a broad altitude range from approximately 200 to 400 km, peaking at ~300 km [*Carr et al.*, 1992]. Unfortunately, high-resolution interferometric observations of the 732 nm emission are limited by the low intensity (maximum ~150 Rayleighs [*Sivjee et al.*, 1999]) and sporadic nature of the $O^+(^2P)$ emissions in nighttime auroras [*Meriwether et al.*, 1974]. In addition, the OH(8, 3) emission at 731.6 nm must be excluded by a suitable optical filter in order to prevent contamination in the $O^+(^2P)$ observations.

[4] The $O(^1D)$ 630 nm and $O^+(^2P)$ 732 nm emissions come from comparable altitudes with $O(^1D) \approx 260 \pm 20$ km [*Kosch et al.*, 2000] and $O^+(^2P) \approx 300 \pm 100$ km [*Carr et al.*, 1992]. Measuring the Doppler shift and broadening of these line emissions gives the line-of-sight velocity and mean temperature of their source, respectively. $O^+(^2P)$ will yield the F-layer ion convection velocity and ion temperature whilst $O(^1D)$ will yield the F-layer neutral wind velocity and neutral temperature. The 630 nm emission has been used extensively for thermospheric research. Independent confirmation of the ion temperatures can be made using incoherent backscatter radar data.

2. Optical Data Analysis

[5] For a detailed description of Fabry-Perot interferometers, the reader is referred to *Hernandez* [1986] and *Vaughan* [1989]. The optical instrument used is an imaging Fabry-Perot interferometer (IFPI) [*Kosch et al.*, 1997a], which uses an image-intensified CCD detector to image up to 3 complete fringes within a 1° field of view. The IFPI is described by *Rees et al.* [1989]. Here we summarize the instrument used in the present study. The capacitance-stabilized etalon has a diameter of 15 cm, a gap of 25 mm and a reflectance of 86%, making it ideal for thermospheric temperature analysis. Since the gap of the etalon can be varied over more than 2 free spectral ranges, the fringes can be optimally placed on the detector. In additional, fringes of a single-mode HeNe laser (632.8 nm) can be scanned across the detector in order to fully define the instrument function. A 5-position filter wheel permits multi-wavelength observations. A 2-axis steering mirror system permits any part of the sky to be viewed. Various gas discharge lamps are routinely used to monitor the IFPI's operational stability. Full technical details of the IFPI are described by *Kosch et al.* [1997b].

[6] The analysis of IFPI fringe images for the purpose of extracting spectral line profiles is well established [e.g. *Nakajima et al.*, 1995; *Kosch et al.*, 1997b]. A thermionic emission (dark) image, which is taken at regular intervals, is subtracted from the fringe image. This image is then flat fielded to remove any spatial non-uniformities in the CCD pixels' response to light. The flat-field image is obtained by illuminating the IFPI with a weak Tungsten lamp through each filter used. The finite width of the filters (0.5–1 nm)

[1]Max-Planck-Institut für Aeronomie, Katlenburg-Lindau, Germany.
[2]Communications Systems, Lancaster University, UK.
[3]Honorary Research Fellow, University of Natal, South Africa.
[4]Physical Sciences, University of Oulu, Finland.

0094-8276/03/2002GL015833$05.00

and the broad continuous spectrum of the lamp ensures that no fringes are produced. The fringe image is then reduced to a line profile in wavelength by integrating pixel intensities in annuli, which are incremented in steps of constant fringe radius squared (equivalent to wavelength). The same procedure is employed for all wavelengths. The exact centre of the circular fringes is determined to sub-pixel resolution by trial and error. This is done by comparing the line profiles taken independently from the four image quadrants. The fringe image centre is automatically adjusted until the four line profiles are identical within the noise error.

[7] The analysis of spectral line profiles for the purpose of extracting thermospheric winds and temperatures is well established [e.g. *Hernandez*, 1978] and is also applicable to emission doublets [e.g. *Connor et al.*, 1993] such as $O^+(^2P)$. Here we briefly describe the analysis procedure used for gas temperature extraction. When an excited thermospheric oxygen atom emits its photon, the line emission will be Doppler shifted according to the bulk velocity of the gas motion, which is usually interpreted as the thermospheric wind speed. In addition, random thermal motion of the emitting oxygen atom will cause a spread in the Doppler shifts along the observing line of sight, which amounts to a broadening of the spectral emission line. The fringe profile of a line emission in an ideal IFPI is represented by a Doppler-broadened Airy function. For a gas in thermal equilibrium, the analytical representation of a Gaussian source profile G(λ, T) follows from the line-of-sight Maxwell-Boltzmann distribution of atom velocities:

$$G(\lambda, T) \propto \exp\left(\frac{-(\lambda-\lambda_o)^2 c^2 m}{2\lambda_o^2 KT}\right)$$

where λ is the Doppler shifted wavelength, λ_o is the rest wavelength, c the speed of light, m is the molecular mass of the emitting atom, K is Boltzmann's constant and T is temperature. Setting

$$G(\lambda, T) = \frac{1}{2}$$

gives

$$\lambda - \lambda_o = \frac{\lambda_o\sqrt{\ln(2)}}{c}\sqrt{\frac{2KT}{m}}$$

[8] The full width at half maximum (FWHM) of the fringe profile is given by

$$\mathrm{FWHM} = 2(\lambda - \lambda_o)$$

[9] Hence, the FWHM is proportional to the square root of the temperature of the emitting gas and all other variables are known quantities.

[10] In practice, a single wavelength at zero Kelvin does not result in an infinitely narrow fringe profile but has a finite width determined by the etalon reflectivity and the sum of all instrumental imperfections. This so-called instrument function $I(\lambda)$ can be determined by illuminating the IFPI with a single-frequency laser (HeNe at 632.8 nm) and is mathematically represented by an Airy function convolved with several specific fringe broadening functions. In practice, this is done for every observing night for a wide range of fringe positions on the detector (equivalent to Doppler shifts). The final data fringe profile $F(\lambda, T)$ is a convolution of $I(\lambda)$ and $G(\lambda, T)$:

$$F(\lambda, T) = \int_{-\infty}^{\infty} G(\varepsilon, T) I(\lambda - \varepsilon)\partial\varepsilon$$

[11] *Hays and Roble* [1971] developed a technique of non-linear fitting the low order Fourier coefficients of an idealized Doppler-broadened instrument function to the observed line profile. However, with modern computers, it is more convenient in practice to convolve the empirically determined $I(\lambda)$ with $G(\lambda, T)$ for various values of T until the best fit is found with the line profile data. Generally, it is not possible to empirically determine $I(\lambda)$ at the same wavelength as the observations $F(\lambda, T)$. We implement the method described by *Killeen and Hays* [1984a] for translating $I(\lambda)$ from the calibration wavelength used (632.8 nm) to the observing wavelengths (630 and 732 nm).

[12] Figure 1 shows an example of the $O^+(^2P)$ doublet wavelength spectrum for the integration period 20:45–20:50 UT on 20th February 2001. Data (diamonds) and fitted model fringe profiles F(λ, T) (solid line) for first and second fringe doublets are shown, giving two estimates of the temperature. Each fringe doublet is fitted with the sum of two Gaussian source profiles G(λ, T), which is convolved with the instrument function I(λ). The nominal doublet separation is 0.08 nm [*Smith et al.*, 1982]. The doublet separation is a free parameter in the fit, giving 0.0797 nm for the first fringe and 0.0796 nm for the second fringe pair. Free spectral range is well defined [*Hernandez*, 1986; *Vaughan*, 1989], giving 0.0107 nm at 732 nm for our IFPI, which is less than the doublet separation. Therefore, the doublet lines are separated by 7.477 orders of interference, which gives an apparent separation of 0.0051 nm in the fringe profile. The relative intensity of the doublet is also a free parameter in the fit, resulting in a ratio of 0.52–0.56 for all the data analysed. The relative doublet intensity coupled to the apparent doublet separation in our IFPI is the reason why one of the line profiles of the doublet appears as a weak perturbation on the right hand shoulder of the dominant line. In the observations described below, the Doppler shift of the $O^+(^2P)$ emission is unknown because the zero velocity baseline could not be determined. This is due to having data only in one pointing direction (north). Hence, the zero wavelength position has been arbitrary chosen.

3. Observations

[13] We present the first ground-based optical observations of ionospheric F-layer ion temperature using the $O^+(^2P)$ emission at 732 nm. The IFPI used is located at Skibotn (69.35°N, 20.36°E), Norway. The IFPI scanned the cardinal positions (north, south, east, west) at 45° elevation angle and the local zenith for 630 nm but observed 732 nm to the north only. An integration time of 300 s for 732 nm and 60 s for 630 nm was used, giving a total cycle time for all positions of ~17 min. The single point measurement for $O^+(^2P)$ was implemented in order to improve the cycle

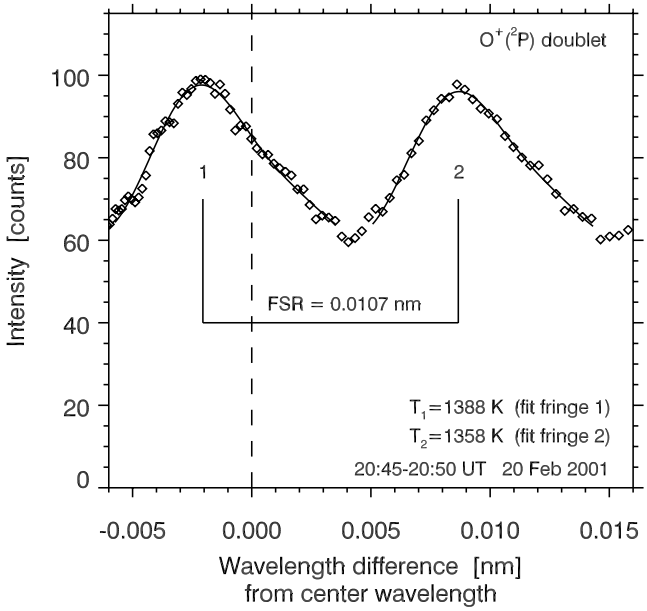

Figure 1. An example of the $O^+(^2P)$ doublet wavelength spectrum for the integration period 20:45–20:50 UT on 20th February 2001. Data (diamonds) and fitted model fringe profiles (solid lines) for first and second fringe doublets are shown.

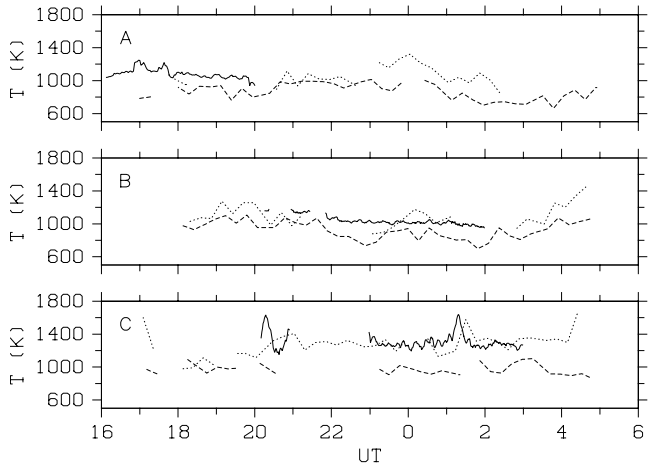

Figure 2. Results from 17th (panel A), 19th (panel B) and 20th (panel C) February 2001. The dashed and dotted curves show the F-layer neutral and ion temperatures from the IFPI, respectively. The solid curve shows the EISCAT ion temperature data for an altitude of 284, 335 and 423 km on the 17th, 19th and 20th February 2001, respectively.

temporal resolution and because previous observations from Skibotn had revealed a lack of data for all the cardinal positions except to the north. Since the IFPI is a passive device, an independent means of determining the emission altitude is required. The incoherent scatter radar facility EISCAT [*Rishbeth and van Eyken*, 1993] is located at Ramfjord (69.59°N, 19.23°E), Norway, about 50 km northwest of Skibotn. The radar routinely measures F-layer ion temperature with 22 km range resolution and a 1–2 min. temporal resolution.

[14] During the period 17–24 February 2001, a campaign of IFPI dual wavelength (630 and 732 nm) measurements was made. On three nights (17, 19 and 20 February 2001) EISCAT was operating, providing independent confirmation of the F-layer ion temperature. Since spatial scanning was not implemented for 732 nm, no IFPI ion vector velocity measurements are possible. Also, EISCAT was pointing mostly along the local magnetic field line (12.8° south zenith angle). Hence, there is a horizontal spatial separation between the optical and incoherent scatter measurement volumes of ~300 km. However, this is not a serious problem for comparison purposes since it was geomagnetically quiet with $Kp \leq 2$ for all the periods of interest. Likewise, the low auroral activity on the selected days greatly reduces the risk of contamination from the first positive N_2 auroral emission bands [Sivjee, private communication].

[15] Figure 2 shows the results from 17 (panel A), 19 (panel B) and 20 (panel C) February 2001. On the 17th, 19th and 20th, Kp was in the ranges 0^+–1, 1^-–2^- and 2^-–2, respectively. The dashed and dotted curves show the F-layer neutral and ion temperatures from the IFPI, respectively. The uncertainty of the measurements is typically <70 K. It is seen that the ion temperature is consistently greater than or equal to the neutral temperature, as expected [e.g. *Killeen et al.*, 1984b; *Cierpka et al.*, 2000; *Kosch et al.*, 2000]. The solid curve shows the EISCAT ion temperature data. The altitude of the radar data was chosen to give the best agreement with the IFPI measurements based on comparing averages for the periods of common data. Figure 3 shows the altitude profile of EISCAT averaged ion temperatures (solid curve) for 19 (panel A) and 20 (panel B) February 2001. The averaged ion temperature from the IFPI is shown by the dotted vertical line. The intersection of the two curves gives the average altitude for the IFPI measurement to the nearest radar range gate (22 km resolution). On the 19th and 20th the 732 nm emission appeared to come from approximately 335 and 423 km altitude, respectively, which is consistent with the expected $O^+(^2P)$ emission altitude [*Carr et al.*, 1992]. There is particularly good agreement between 23 and 03 UT on 20

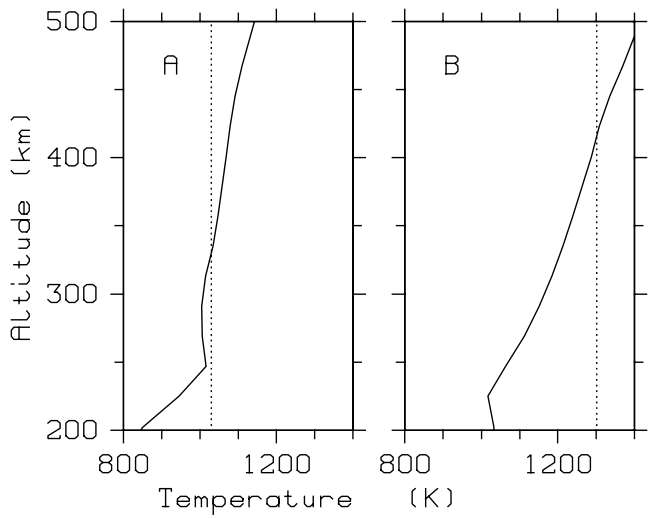

Figure 3. The altitude profile of average EISCAT ion temperature (solid curve) for 19th (panel A) and 20th (panel B) February 2001. The average FPI ion temperature (dotted line) is also shown.

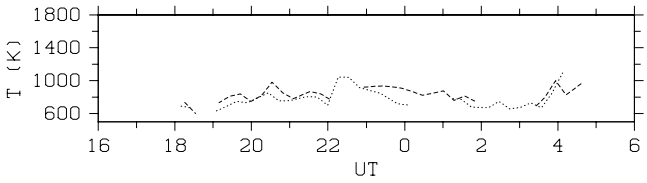

Figure 4. Results from 24th February 2001. The dashed and dotted curves show the F-layer neutral and ion temperatures from the IFPI, respectively.

February 2001 (Figure 2, panel C). The small time shift is presumably due to the ~300 km spatial separation between the measurement volumes. The overlap of IFPI and EISCAT data on 17 February 2001 is very limited, making this height estimate uncertain. The apparent IFPI measurement altitude was ~284 km.

[16] For the selected altitudes and periods of overlapping data, the average ion temperature from the IFPI and EISCAT are 1041 and 1084 K on the 17th, 1030 and 1033 K on the 19th, and 1301 and 1308 K on 20 February 2001, respectively. The average IFPI neutral and ion temperatures for the entire data sets are 867 and 1058 K on the 17th, 928 and 1098 K on the 19th, and 979 and 1277 K on 20 February 2001, respectively, which is consistent with previous results [*Cierpka et al.*, 2000; *Kosch et al.*, 2000].

[17] Figure 4 shows the IFPI data for 24 February 2001 in the same format as Figure 2. On this day Kp was in the range $0-0^+$. No EISCAT data was available. The average neutral and ion temperatures for the entire measurement period are 831 and 777 K, respectively. Indeed, the ion temperature is lower than the neutral temperature for most of the time, which is unrealistic. Presumably, this is due to the $O^+(^2P)$ auroral emission altitude being below the $O(^1D)$ airglow altitude. This anomalous result demonstrates that the variable altitude for the 732 nm emission (>100 km) limits the usefulness of the optical method of F-layer ion temperature measurement.

4. Conclusion

[18] We show the first optical measurements of high-latitude F-layer ion temperatures. We also demonstrate that these observations are consistent with incoherent scatter radar data and the expected altitude of the $O^+(^2P)$ emission. Unfortunately, the variable emission altitude may make interpretation of the results difficult. In order to study this problem more closely further optical and incoherent scatter measurements with both instruments observing in a common volume need to be undertaken.

[19] **Acknowledgments.** EISCAT is an international scientific association supported by the research councils of Finland (SA), France (CNRS), Germany (MPG), Japan (NIPR), Norway (RCN), Sweden (NFR) and the United Kingdom (PPARC).

References

Carr, S. S., T. L. Killeen, and W. R. Coley, Remote-sensing observations of F-region ion drift velocities using Dynamics Explorer-2 Doppler measurements of the $O^+(^2P)$ λ 732.0 nm emission, *Geophys. Res. Lett.*, *19*, 1455–1458, 1992.

Cierpka, K., M. J. Kosch, M. Rietveld, K. Schlegel, and T. Hagfors, Ion-neutral coupling in the high-latitude F-layer from incoherent scatter and Fabry-Perot interferometer measurements, *Ann. Geophys.*, *18*, 1145–1153, 2000.

Connor, J. F., R. W. Smith, and G. Hernandez, Techniques for deriving Doppler temperatures from multiple-line Fabry-Perot profiles: an analysis, *Appl. Opt.*, *32*, 4437–4444, 1993.

Hays, P. B., and R. G. Roble, A technique for recovering Doppler line profiles from Fabry-Perot interferometer fringes of very low intensity, *Appl. Opt.*, *10*, 193–200, 1971.

Hernandez, G., Analytical description of a Fabry-Perot spectrometer. 4: Signal noise limitations in data retrieval; winds, temperature, and emission rate, *Appl. Opt.*, *17*, 2967–2972, 1978.

Hernandez, G., Fabry-Perot Interferometers, Cambridge Studies in Modern Optics (Vol 3), Cambridge University Press, 1986.

Killeen, T. L., and P. B. Hays, Doppler line profile analysis for a multichannel Fabry-Perot interferometer, *Appl. Opt.*, *23*, 612–620, 1984a.

Killeen, T. L., P. B. Hays, G. R. Carignan, R. A. Heelis, W. B. Hanson, N. W. Spencer, and L. H. Brace, Ion-Neutral Coupling in the High-Latitude F Region: Evaluation of Ion Heating Terms From Dynamics Explorer 2, *J. Geophys. Res.*, *89*, 7495–7508, 1984b.

Kosch, M. J., T. Hagfors, and D. Rees, A new Fabry-Perot Interferometer Experiment for Atmospheric Studies with the EISCAT Incoherent Backscatter Radar, *Adv. Space Res.*, *20*(6), 1133–1136, 1997a.

Kosch, M. J., A. Kohsiek, K. Schlegel, and T. Hagfors, A new Fabry-Perot Interferometer Experiment for Neutral Atmosphere Studies in Conjunction with the EISCAT Incoherent-Backscatter Radar System, Max-Planck-Institut für Aeronomie Technical Report (MPAE-T-010-97-20), 1997b.

Kosch, M. J., M. Ishii, S. Nozawa, D. Rees, K. Cierpka, A. Kohsiek, K. Schlegel, R. Fujii, T. Hagfors, T. J. Fuller-Rowell, and C. Lathuillere, A Comparison of Thermospheric Winds and Temperatures from Fabry-Perot Interferometer and EISCAT Radar Measurements with Models, *Adv. Space Res.*, *26*(6), 979–984, 2000.

Meriwether, J. W., P. B. Hays, K. D. McWatters, and A. F. Nagy, Interferometric measurements of the λ 7319 Å doublet emissions of OII, *Planet. Space Sci.*, *22*, 636–638, 1974.

Nakajima, H., S. Okano, H. Fukunishi, and T. Ono, Observations of thermospheric wind velocities and temperatures by use of a Fabry-Perot Doppler imaging system at Syowa Station, Antarctica, *Appl. Opt.*, *34*, 8382–8395, 1995.

Omholt, A., The red and near-infrared auroral spectrum, *J. Atmos. Terr. Phys.*, *10*, 320, 1957.

Rees, D., I. McWhirter, A. Aruliah, and S. Batten, Upper Atmospheric Wind and Temperarure Measurements using Imaging Fabry-Perot Interferometers, WITS Handbook (Vol 2), edited by C. H. Lui, 188–223, 1989.

Rishbeth, H., and A. P. van Eyken, EISCAT: Early History and the First Ten Years of Operation, *J. Atmos. Terr. Phys.*, *55*, 525–542, 1993.

Sivjee, G. G., G. J. Romick, and M. H. Rees, Intensity ratio and center wavelengths of [OII] (7320–7330 Å) line emissions, *Astrophys. J.*, *229*, 432–438, 1979.

Sivjee, G. G., D. Shen, J.-H. Yee, and G. J. Romick, Variations, with peak emission altitude, in auroral O_2 atmospheric (1, 1)/(0, 1) ratio and its relation to other auroral emissions, *J. Geophys. Res.*, *104*, 28,003–28,018, 1999.

Smith, R. W., G. G. Sivjee, R. D. Stewart, F. G. McCormac, and C. S. Deehr, Polar Cusp Ion Drift Studies Through High-Resolution Interferometry of O^+ 7320-Å Emission, *J. Geophys. Res.*, *87*, 4455–4460, 1982.

Smith, R. W., K. J. Winser, A. P. van Eyken, S. Quegan, and B. T. Allen, Observation and theoretical modelling of a region of downward field-aligned flow of O^+ in the winter dayside polar cap, *J. Atmos. Terr. Phys.*, *47*, 489–495, 1985.

Vaughan, J. M., The Fabry-Perot Interferometer: History, Theory, Practice and Applications, Adam Hilger, Bristol, UK, 1989.

K. Cierpka and T. Hagfors, Max-Planck-Institut für Aeronomie, Max-Planck-Str. 2, 37191 Katlenburg-Lindau, Germany.

A. J. Kavanagh and M. J. Kosch, Communication Systems, Lancaster University, Lancaster, LA1 4YR, UK.

H. Holma, Physcial Sciences, University of Oulu, FIN-90014, Oulu, Finland.